

## CARS Spectra of Thermally Excited SF<sub>6</sub> Molecules

A. A. Puretzky

Institute of Spectroscopy, Academy of Sciences, Troizk, SU-142092 Moscow, USSR

V. N. Zadkov

Moscow State University

Received 5 October 1982/Accepted 11 February 1983

**Abstract.** CARS spectra of the  $\nu_1$  mode of thermally excited SF<sub>6</sub> were calculated numerically. The influence of the vibrational quasicontinuum on the CARS spectra has been considered by introducing different types of the homogeneous broadening at different vibrational levels. The appearance of additional lines in the CARS spectrum due to mixing of high-lying vibrational levels by Fermi coupling was considered numerically in the frame of a simple model. A comparison of calculated and experimental spectra has been made.

**PACS:** 82.50, 33

The methods of coherent probing of vibrationally excited molecules, and CARS in particular, have been used in studies of multiple-photon excitation of molecules by infrared laser radiation [1, 2]. Similar to many other probing techniques like uv absorption [3], ir-absorption [4], ir luminescence [5], spontaneous Raman scattering [6] the CARS technique permits one to analyse the distribution of vibrationally excited molecules. The basic advantages of CARS probing compared with the above-mentioned spectroscopic methods are excellent spatial and spectral resolution. Another important feature of CARS probing is the sensitivity of the CARS signal with respect to the value of homogeneous broadening of the probed transition. The influence of this broadening might be understood qualitatively, considering the harmonic oscillator. The intensity of the anti-Stokes signal  $I_a$  in CARS is determined by the value of the third-order nonlinear susceptibility of the sample  $\chi^{(3)}$  and by the intensities of the probing beams  $I_1$  and  $I_2$  [7]:

$$I_a(2\omega_1 - \omega_2) \sim |\chi^{(3)}(2\omega_1 - \omega_2)|^2 I_1^2 I_2. \quad (1)$$

In the simplest case of a harmonic oscillator, when the difference of the probing frequencies  $\omega_1, \omega_2$  coincides with the vibrational frequency  $\Omega$ , i.e.  $\omega_1 - \omega_2 = \Omega$ , the scattered radiation intensity integrated over vibration-

al states will be determined by its susceptibility:

$$\chi_{\text{int}}^{(3)} \sim \sum_{v=1}^{\infty} \frac{v(N_{v-1} - N_v)}{\Gamma_v}, \quad (2)$$

where  $\Gamma_v$  is the homogeneous width of the transition  $v-1 \rightarrow v$ . If  $\Gamma_v$  does not depend on  $v$ ,

$$\chi_{\text{int}}^{(3)} \sim \sum_{v=0}^{\infty} N_v = N. \quad (3)$$

In this latter case the integral intensity does not depend on the distribution function over vibrational states and is determined only by the total number of molecules,  $N$ . It can be easily seen from (2) and (3) that any rise of  $\Gamma_v$  with a rise of vibrational level  $v$  will lead to a decrease of the integral intensity at the center of the CARS band as  $|\chi^{(3)}|^2 \sim \Gamma_v^{-2}$ . For highly excited vibrational states of polyatomic molecules the anharmonic coupling (for example, the Fermi resonances) will lead to the formation of homogeneously broadened vibrational bands (vibrational quasicontinuum). The widths of these bands grow with an increase of the vibrational energy content  $E_v$  in the molecule. Therefore, similar to the harmonic oscillator case, there should be significant influence of  $\Gamma_v(E_v)$  on the CARS spectrum of excited molecules.

In this paper we consider, by numerical calculation, the influence of homogeneous broadening in the vibrational quasi-continuum region on the CARS spectrum of the fully symmetric mode  $\nu_1$  of the SF<sub>6</sub> molecule. It has been shown that by comparing the calculated and experimental spectra it is possible to judge about the value and the behaviour of  $\Gamma_\nu(E_\nu)$ .

### 1. Calculation of the CARS Spectrum

A detailed description of the CARS process can be found in a number of reviews [7, 8]. In three-wave mixing of the pump wave at  $\omega_1$  and of the Stokes wave at  $\omega_2$  a new wave is generated in the anti-Stokes region at  $\omega_a = 2\omega_1 - \omega_2$ . The intensity of this wave is given by (1). The third-order nonlinear susceptibility contains a nonresonant term  $\chi_{nr}^{(3)}$  plus contributions from the transitions  $i \rightarrow f$  with the frequencies  $\omega_{if} = (E_f - E_i)/hc$  and with the width of the Raman line (HWHM)  $\Gamma_{if}$ :

$$\chi^{(3)} = \chi_{nr}^{(3)} + \sum_{if} A(N_i - N_f) \left( \frac{d\sigma}{d\Omega} \right)_{if} \frac{1}{\omega_{if} - (\omega_1 - \omega_2) - i\Gamma_{if}}, \quad (4)$$

where  $A$  is a constant which is independent of frequency,  $N_i$  and  $N_f$  are the populations of the initial and final states,  $(d\sigma/d\Omega)_{if}$  is the spontaneous Raman scattering cross-section. Let us consider a particular case of the CARS spectrum of the fully symmetric mode  $\nu_1$  of SF<sub>6</sub> molecules. In this case

$$f = \langle v_1 + 1, v_i, J' | \leftarrow i = \langle v_1, v_i, J \rangle, \quad (5)$$

where  $\{v\} = \{v_1, v_2, \dots, v_6\}$  are the vibrational quantum numbers of the modes  $\nu_1, \nu_2, \dots, \nu_6$  of the SF<sub>6</sub> molecule, and  $J, J'$  are the rotational substates of the  $\nu_1$  mode.

In the CARS process the selection rules for rotational quantum numbers are identical to those for the spontaneous Raman process

$$\left( \frac{d\sigma}{d\Omega} \right)_{\nu_1} \sim \begin{pmatrix} J' & \kappa & J \\ -K' & \tau & K \end{pmatrix}^2, \quad (6)$$

where  $\kappa$  and  $\tau$  are the rank and the component index of the spherical polarizability tensor  $\alpha(\kappa, \tau)$ . For spherical top molecules  $J = K$  is fulfilled. Since for the considered case of the totally symmetric mode  $\nu_1(A_{1g})$  of the SF<sub>6</sub> molecule (point group O<sub>h</sub>) the Raman transitions appear only due to the scalar part of the polarizability  $\alpha(0, 0)$ , i.e.  $\kappa = 0, \tau = 0$ ; the 3- $j$  symbol in (6) will differ from zero only when  $J' - J = 0$ . This means that for any transition (5) the CARS spectrum will consist only of Q-branches ( $\Delta J = 0$ ).

In the case of the Boltzmann distribution of molecules over vibrational and rotational states at the tempera-

ture  $T$  for the resonant part of the susceptibility we have

$$\chi_r^{(3)} = A \sum_{\{v\}} \sum_J P_{\{v\}} N_{\{v\}} \left\{ 1 - \exp \left[ \frac{-hc(\omega_{\{v\}} + \omega_J)}{kT} \right] \right\} \cdot \frac{P_J N_J}{\omega_{\{v\}} + \omega_J - (\omega_1 - \omega_2) - i\Gamma_{\{v\}}}. \quad (7)$$

Here

$$\omega_{\{v\}} = \frac{E(v_1 + 1, v_2, \dots, v_6) - E(v_1, v_2, \dots, v_6)}{hc} = \omega_0 + 2X_{11}v_1 + \sum_{i=1}^6 X_{1i}v_i, \quad (8)$$

where  $\omega_0$  is the transition frequency  $\langle v_1 = 1, v_i = 0 | \leftarrow \langle v_1 = 0, v_i = 0 |$ , and  $X_{ij}$  are the anharmonicity constants. We shall take the harmonic approximation for the probability of vibrational transition  $P_{\{v\}}$

$$P_{\{v\}} = v_1 + 1. \quad (9)$$

The population of the  $\{v\}$ <sup>th</sup> vibrational state is given by

$$N_{\{v\}} = \frac{g_{\{v\}} \exp(-E_{\{v\}}/kT)}{\sum_{\{v\}} g_{\{v\}} \exp(-E_{\{v\}}/kT)}, \quad (10)$$

where

$$g_{\{v\}} = \frac{1}{16}(v_2 + 1) \prod_{i=3}^6 (v_i + 1)(v_i + 2), \quad (11)$$

is the degeneracy of the state  $\{v\}$ , and

$$E_{\{v\}} = \sum_{i=1}^6 hc\omega_i v_i. \quad (12)$$

The population of the  $J$ <sup>th</sup> rotational sublevel is given by

$$N_J = \frac{(2J + 1)^2 \exp[-B_{\{v\}}hcJ(J + 1)/kT]}{\sum_J (2J + 1)^2 \exp[-B_{\{v\}}hcJ(J + 1)/kT]}, \quad (13)$$

and  $P_J = 1$  for Q-branch transitions. The frequencies of the rotational lines in the Q-branch will be determined by the difference of rotational constants  $\Delta B_{\{v\}}$  for the vibrational transition under consideration:

$$\Delta\omega_J^Q = \Delta B_{\{v\}}J(J + 1). \quad (14)$$

For the case of  $\nu_1$  mode excitation we have  $\Delta B_{\{v\}} = \Delta B_{\nu_1}$ .

### 2. Spectroscopic Constants

The calculation of the CARS spectrum in the approximation (8–14) demands knowledge of the following spectroscopic constants: the frequencies of normal

Table 1<sup>a</sup>

	<i>i</i> =1	<i>i</i> =2	<i>i</i> =3	<i>i</i> =4	<i>i</i> =5	<i>i</i> =6
$\nu_i$	774.5445(10) <sup>b</sup>	643.35 ± 0.01 <sup>c</sup>	947.9763307(62) <sup>d</sup>	615.025 <sup>e</sup>	523.5 ± 0.1 <sup>c</sup>	347.0 ± 0.1 <sup>c</sup>
$X_{i1}$	-0.8677 ± 0.03 <sup>b</sup>					
$X_{i2}$	-2.44 ± 0.2 <sup>c</sup>	-0.4 ± 0.3 <sup>f</sup>				
$X_{i3}$	-2.9308 ± 0.03 <sup>b</sup>	-2.0 ± 0.6 <sup>f</sup>	-1.83 <sup>g</sup>			
$X_{i4}$	-1.08 ± 0.02 <sup>c</sup>	-1.22 ± 0.02 <sup>h</sup>	-1.53 ± 0.02 <sup>h</sup>	0.12 ± 0.02 <sup>h</sup>		
	-1.03 ± 0.02 <sup>h</sup>					
$X_{i5}$	-1.15 ± 0.02 <sup>c</sup>	-0.7 ± 0.1 <sup>c</sup>	-0.5 ± 1.0 <sup>f</sup>	-0.37 ± 0.02 <sup>h</sup>	-0.5 ± 1.0 <sup>f</sup>	
$X_{i6}$	-0.38 ± 0.02 <sup>c</sup>	-0.35 ± 0.05 <sup>c</sup>	-1.0 ± 0.1 <sup>f</sup>	-0.11 ± 0.02 <sup>h</sup>	-0.5 ± 1.0 <sup>f</sup>	-0.1 ± 0.1 <sup>c</sup>
$B_v$	0.09111 <sup>h</sup>					
$\Delta B_{v_1}$	-1.1038(4) · 10 <sup>-4</sup> <sup>b</sup>					

<sup>a</sup>All values are given in cm<sup>-1</sup>

<sup>b</sup>[12], <sup>c</sup>[9], <sup>d</sup>[17], <sup>e</sup>[11], <sup>f</sup>[18], <sup>g</sup>[19], <sup>h</sup>[10]

vibrations  $\nu_i$ , anharmonic constants  $X_{1i}$ , rotational constants  $B_{(v)}$  and difference of the rotational constants  $\Delta B_{v_1}$ . All necessary data are given in Table 1. The frequencies of the normal vibrations and the anharmonicity constants for SF<sub>6</sub> are known with good accuracy from the analysis of spontaneous Raman spectra [9], and from high-resolution semiconductor laser ir spectroscopy of the fundamental bands and overtones of SF<sub>6</sub> [10–12]. For the rotational constant we took its equilibrium value  $B_e$ . The difference of the rotational constants,  $\Delta B_{v_1}$ , was estimated in [13] on the basis of stimulated Raman gain measurements of the  $\nu_1$  mode of SF<sub>6</sub>. Esherick and Owyong [13] did not observe octahedral splittings in  $\nu_1$  that makes it possible to use the simplest approximation (14) for  $\omega_J^2$ . The value of the nonresonant part of the third-order nonlinear susceptibility  $\chi_{nr}^{(3)}$  was estimated in [14] and is equal to  $(5.3 \pm 3.1) \times 10^{-18}$  cm<sup>3</sup> erg<sup>-1</sup>. The comparison of the absolute values of  $\chi_r^{(3)}$  and  $\chi_{nr}^{(3)}$  shows that in our case the nonresonant part of the susceptibility can be neglected since  $\chi_{nr}^{(3)}/\chi_r^{(3)} = 10^{-5}$ . The detailed analysis of the influence of laser line shapes in the case of narrow-band CARS and of the spectrometer slit function for broad-band CARS experiments have been done in [15]. In our calculation we used concrete parameters which correspond to the experiment described in [1]. The calculation of the CARS spectrum was done numerically according to (8–14) taking into account all rotational-vibrational levels which are populated at a given temperature. In each given case the values  $\{v_{max}\}$  and  $E_v^{max}$ , where the calculation was cut-off, were chosen by estimating the influence of these parameters on the calculated CARS spectrum.

### 3. Results

Figure 1a–e shows the result of calculations of CARS spectra ( $|\chi^{(3)}|^2$ ), imaginary part of susceptibility

$\text{Im}\{\chi^{(3)}\}$  and its real part  $\text{Re}\{\chi^{(3)}\}$ , respectively. The calculations were performed with the assumption that the homogeneous linewidth of the vibrational transitions  $\Gamma_v(E_v)$  does not depend on  $\{v\}$  and is equal to 0.2 cm<sup>-1</sup>. As the temperature or the average vibrational energy of the molecules  $E_v$  grows the CARS spectra are shifted to the red from the band corresponding to the transition  $\langle v_1=0, v_i=0 | \leftarrow \langle v_1=1, v_i=0 \rangle$ , and become broader. The fast fall of the CARS intensity at the maximum is apparent. These spectral changes are due to anharmonicity, (8), and rotational broadening of the  $Q$ -branches corresponding to each vibrational transition (13).

The influence of homogeneous broadening on the shape of the considered CARS band was calculated under the assumption of different models for the dependence  $\Gamma_v(E_v)$ . At the present time the behaviour of  $\Gamma_v(E_v)$  at the onset of the vibrational quasicontinuum is not known. To understand the influence of  $\Gamma_v$  on CARS spectra, the calculations were performed for the simplest cases of  $\Gamma_v(E_v)$  at the onset of the vibrational quasicontinuum. The position of the quasicontinuum onset  $E_q$  and the value of  $\Gamma_v$  were varied. Figure 2a and b show the CARS spectra of the  $\nu_1$  mode of SF<sub>6</sub> in the case when  $\Gamma_v$  is switched at  $E_q$  in a stepwise way from 0.2 cm<sup>-1</sup> to its final value 1 cm<sup>-1</sup> (Fig. 2a) or 5 cm<sup>-1</sup> (Fig. 2b). The calculations were done for  $T=1000$  K when the average vibrational energy is equal to  $\bar{E}_v=6570$  cm<sup>-1</sup>. The case  $\Gamma_v=\text{const}=0.2$  cm<sup>-1</sup> is shown in Fig. 2a and b by dotted lines (Fig. 1a). Depending on the position of the quasicontinuum onset  $E_q$  and the value of the homogeneous broadening the influence of this broadening on the CARS spectra is different. Thus, for  $\Gamma_v=1$  cm<sup>-1</sup> (Fig. 2a) the broadening of the spectrum at low onset  $E_q=4000$  cm<sup>-1</sup> as well as its narrowing at large  $E_q$  are observed. For  $\Gamma_v=5$  cm<sup>-1</sup>, a significant narrowing and deformation of the spectrum is seen (Fig. 2b). The observed variations of the shape of the CARS spectra are due to the in-

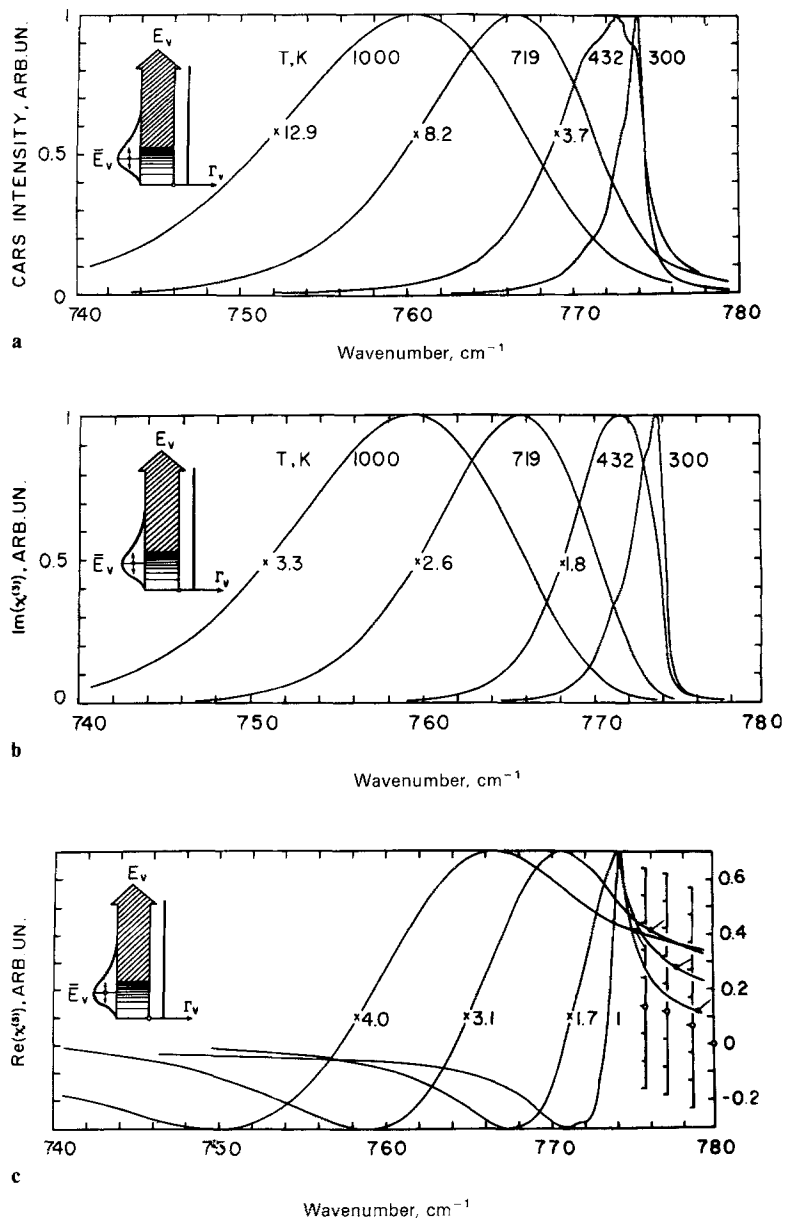


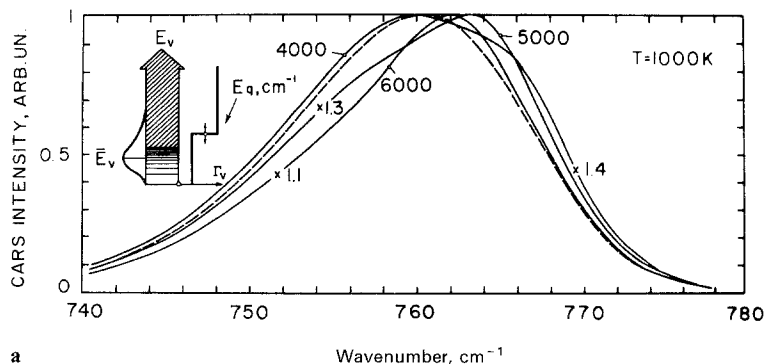
Fig. 1a-c. Computer plots of (a)  $|\chi^{(3)}|^2$  CARS spectrum, (b)  $\text{Im}\{\chi^{(3)}\}$ , (c)  $\text{Re}\{\chi^{(3)}\}$  for the  $\nu_1$  mode of  $\text{SF}_6$  at different temperatures. The homogeneous width is assumed to be independent of  $E_v$  and equal to  $0.2 \text{ cm}^{-1}$  (see insert). The factors show the ratio of the curve maximum at 300 K to that of the corresponding curve. The position of the zero level for every  $\text{Re}\{\chi^{(3)}\}$  curve in (c) is shown by a set of respective axis

fluence of two factors: i) addition of a homogeneous width  $\Gamma_v$  to inhomogeneous broadening, which forms the observed contour and ii) a decrease due to  $\Gamma_v$  of the integral intensity of individual Q-branches corresponding to transitions from high-lying vibrational states  $E_v \geq E_q$ . Introduction of homogeneous broadening in the form of a step function gives rise to a maximum in the blue. This maximum is smoothed considerably if the homogeneous broadening is switched monotonically. Figure 3 shows the changes in CARS spectra with temperature of the  $\text{SF}_6$  gas or its average vibrational energy  $E_v$ . The spectrum was calculated under the assumption of "monotonically" increased  $\Gamma_v$  from its minimum value  $0.2 \text{ cm}^{-1}$  for  $E_q \leq 5000 \text{ cm}^{-1}$  up to  $2 \text{ cm}^{-1}$  for  $E_q \geq 6000 \text{ cm}^{-1}$ . The behaviour of  $\Gamma_v$  as-

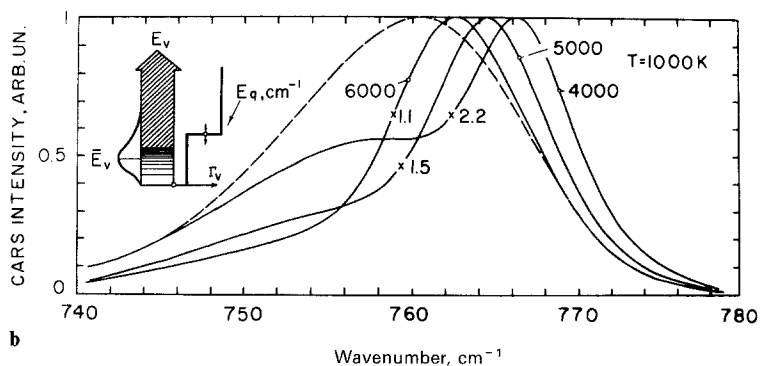
sumed in this calculation is shown in the insert of Fig. 3.

#### 4. Inhomogeneous Broadening due to Mixing of Harmonic States

The above-mentioned calculations of CARS spectra were made without taking into account the anharmonic splitting of the degenerate vibrational states  $\langle v|$ , (12). Such an approach is justified if mixing of anharmonically split sublevels  $\langle v, \alpha|$  due to anharmonic coupling (Fermi resonances) is not taken in account. Due to orthogonality of the wave functions for anharmonically split sublevels  $\langle v_1, v_2, \alpha|$  and  $\langle v_1 + 1, v_2, \alpha'|$



a



b

Fig. 2a and b. Computed CARS spectra of the  $\nu_1$  mode of SF<sub>6</sub> with the introducing of a homogeneous broadening at different quasicontinuum onsets  $E_q = 4000, 5000, 6000 \text{ cm}^{-1}$ .  $\Gamma_v$  was varied in a stepwise way from  $0.2 \text{ cm}^{-1}$  to (a)  $1 \text{ cm}^{-1}$  and (b)  $5 \text{ cm}^{-1}$  at the  $E_q$  level (see insert). The spectra was calculated at  $T = 1000 \text{ K}$  ( $\bar{E}_v = 6570 \text{ cm}^{-1}$ ). The dashed line shows a computed CARS spectrum with  $\Gamma_v = 0.2 \text{ cm}^{-1}$  (Fig. 1a) for comparison. The factors show the ratio of the maximum of the dashed curve to the one of the respective curve

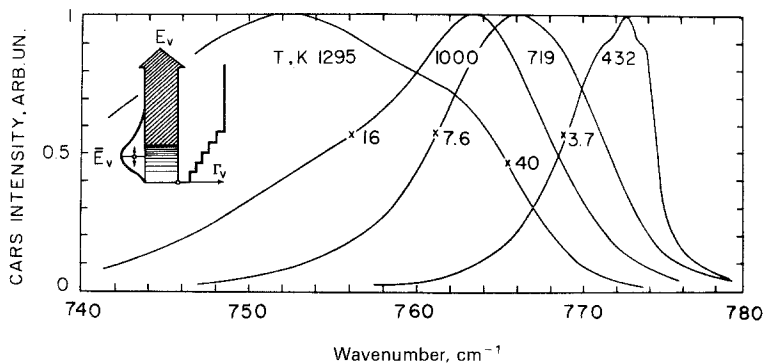


Fig. 3. Computed CARS spectra of the  $\nu_1$  mode of SF<sub>6</sub> at different temperatures with the introducing of a homogeneous broadening.  $\Gamma_v$  increases monotonically from minimum value  $0.2 \text{ cm}^{-1}$  for  $E_q \leq 5000 \text{ cm}^{-1}$  up to  $2 \text{ cm}^{-1}$  for  $E_q \geq 6000 \text{ cm}^{-1}$ . The factors show the ratio of the curve maximum at  $T = 1000 \text{ K}$  for  $\Gamma_v = \text{const}$  (Fig. 1a) to the one of the respective curve

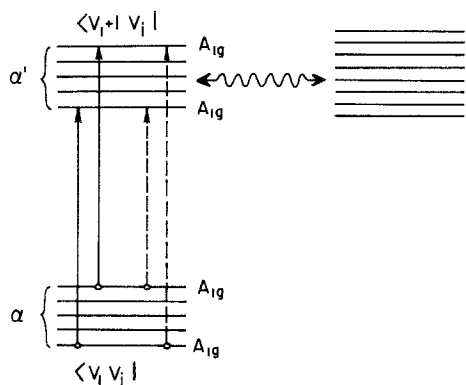


Fig. 4. The appearance of shifted components in CARS spectra due to Fermi resonances

the transitions, in the CARS spectrum, are allowed between sublevels of the same symmetry only if  $\alpha = \alpha'$ , i.e. all the transitions of this type will occur at the same resonance frequency. Mixing of the sublevels  $\alpha$ , due to Fermi interaction with other modes, the transitions between the states  $\alpha \rightarrow \alpha'$  that have the same symmetry will be allowed. Therefore the CARS spectrum will have components detuned to the both sides from the resonant frequency and the spacing between them will be equal to the width of split zone  $\alpha$ . The appearance of these detuned components is illustrated in Fig. 4. In case of the SF<sub>6</sub> molecule the strongest Fermi resonance is the four-frequency resonance  $\nu_1 + \nu_5 \approx \nu_3 + \nu_6$  with the detuning of  $\Delta \approx 3 \text{ cm}^{-1}$ .

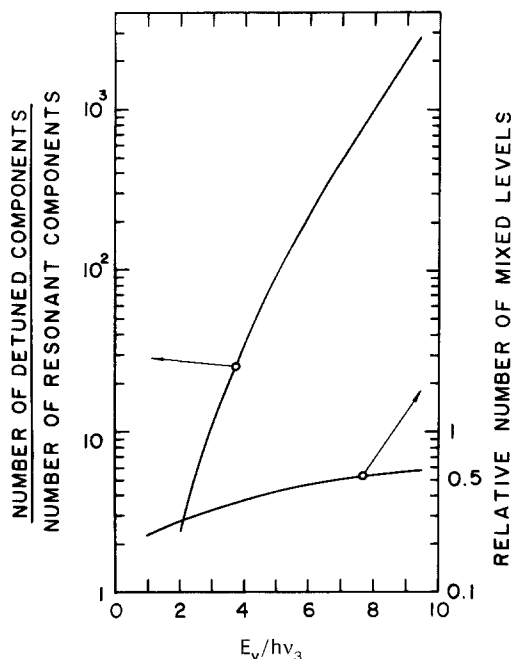


Fig. 5. The relative number of mixed levels due to Fermi resonance  $\nu_1 + \nu_5 \approx \nu_3 + \nu_6$  for  $\text{SF}_6$  (right scale) and the ratio of the number of detuned components to the number of resonant components (left scale) versus vibrational energy  $E_v$ .

Therefore, the anharmonically split components  $\langle \alpha |$  of all states  $\langle v, \alpha |$  for which  $v_3 \neq 0, v_6 \neq 0$  and also  $v_3 = 0, v_6 = 0, v_5 \neq 0$  will be mixed due to Fermi interaction. Figure 5 shows the calculated dependence of the number of states, which are mixed by the above-discussed mechanism versus vibrational energy level  $E_v$ . The number of interacting states grows slowly with  $E_v$ . For  $\bar{E}_v \approx 6000 \text{ cm}^{-1}$  approximately half vibrational states are mixed. To evaluate the relative number of detuned and resonant components, the computer program took into account the expansion of each state  $\langle v |$  to irreducible representations. In accordance with the selection rules for CARS spectra the number or re-

sonant components  $n_{\text{res}}$  are equal to

$$n_{\text{res}} = \sum_i \kappa_i,$$

where  $\kappa_i$  is the number of states of  $I_i$  type, and the summation is performed over all possible types of the  $O_h$  point group. The number of detuned components  $n_{\text{det}}$  (Fig. 4) is determined by the transitions between arbitrary states of the same symmetry, and therefore

$$n_{\text{det}} = \sum_i (\kappa_i)^2 - \kappa_i.$$

The dependence  $n_{\text{det}}/n_{\text{res}}$  versus  $E_v$  is shown in Fig. 5. The computational results (Fig. 5) show that even for relatively low excitation levels ( $E_v \geq 3000 \text{ cm}^{-1}$ ) the inhomogeneous broadening due to Fermi mixing of anharmonically split substates can influence the CARS spectrum of the  $\nu_1$  mode of  $\text{SF}_6$ .

The detailed calculation of inhomogeneous broadening of this type and the bandshape corresponding to a single vibrational transition cannot be made since the necessary spectroscopic parameters for high-lying vibrational states are unknown. Therefore the inhomogeneous broadening considered above was taken into account in a simplified model. A boundary for  $E_v$  was introduced, above which each Q-branch was split into 5 components while the integral intensity of the spectrum was remained the same. With this assumption, in accordance with calculations for the number of interacting vibrational states (Fig. 5), half of the vibrational transitions had a split Q-branch. Figure 6 shows the result of these calculations. Here the splitting of the Q-branches was introduced at  $E_v \geq 5000 \text{ cm}^{-1}$  and the value of splitting was taken as  $2 \text{ cm}^{-1}$ . It can be seen that the qualitative character of the variation of the CARS spectrum bandshape is the same as in the case of a similar introduction of homogeneous broadening.

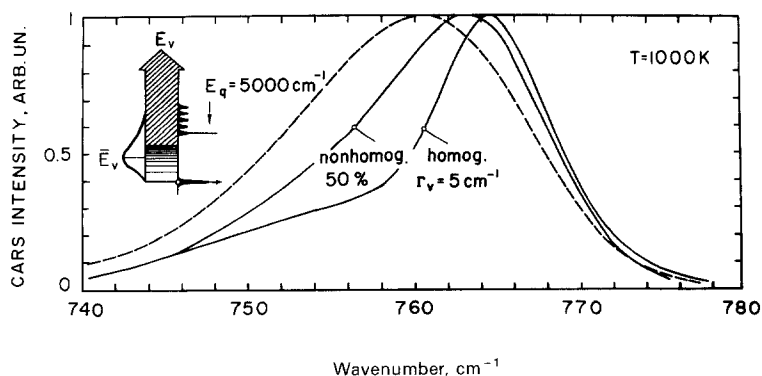


Fig. 6. The influence of inhomogeneous broadening due to Fermi resonances of the CARS spectrum of  $\text{SF}_6$ . In accordance with the number of mixed levels (Fig. 5) each Q-branch for 50% of all transitions was split in five components with the full width  $2 \text{ cm}^{-1}$  at  $E_q = 5000 \text{ cm}^{-1}$  (see insert). The spectrum with  $\Gamma_v = 0.2 \text{ cm}^{-1}$  at  $T = 1000 \text{ K}$ . (Fig. 1a) (dashed line) and the spectrum with  $\Gamma_v = 5 \text{ cm}^{-1}$  (Fig. 2b) are shown for comparison

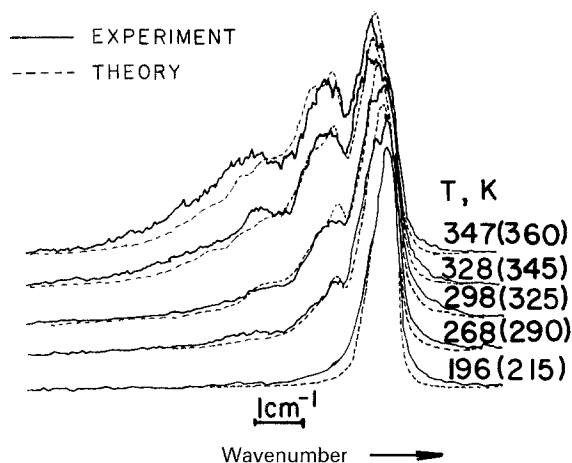


Fig. 7. Comparison of the calculated spectra with the experimental results of [16] in the temperature range of 196–347 K.

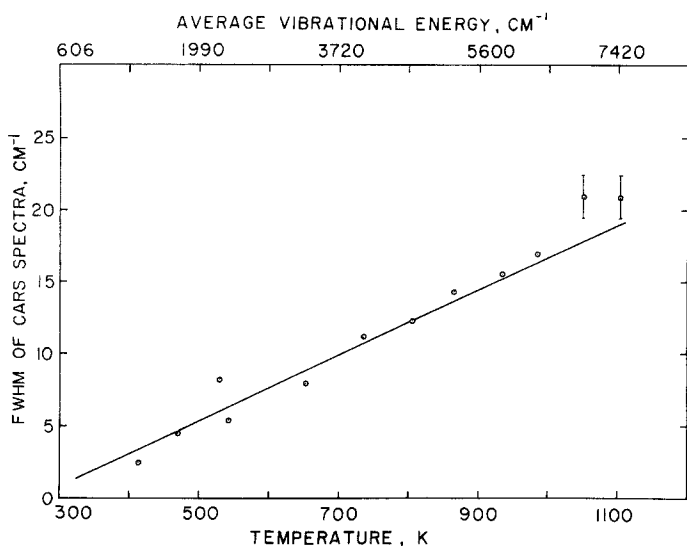


Fig. 8. The experimental (points) [1] and calculated (solid line) dependence of the CARS spectrum (FWHM) versus the SF<sub>6</sub> gas temperature

## 5. Comparison with Experiment

At the present time there are only few publications on the bandshape of the CARS spectrum for the  $\nu_1$  mode of SF<sub>6</sub> at room temperature [1, 14, 16]. The computation of the CARS spectrum, that was performed in this paper agreed fairly well at 300 K with the experimental results given in [1, 14, 16]. Figure 7 shows experimental CARS spectra of SF<sub>6</sub> reported in [16] in the narrow temperature range 196–347 K. The results of our numerical calculations are shown by the dotted lines. The calculated spectra are in good agreement

with the experimental results at temperatures which are slightly different from those reported in [16]. These temperatures are given in brackets in Fig. 7. The apparent small disagreement may be due to the impossibility in this work to take into account the real shape of the instrumental functions.

Analysis of CARS spectra at elevated temperatures ranging from 300 to 1000 K was performed in [1]. Figure 8 shows the dependence of the width (FWHM) of the considered band of the CARS spectrum versus the gas temperature [1]. The solid line shows the computational results under the assumption of  $\Gamma_v = \text{const}$ , taking into account the instrumental parameters reported in [1]. It may be seen that up to average vibrational energies  $\bar{E}_v \approx 6000 \text{ cm}^{-1}$  the calculated results are in good agreement with the experiment. The performed comparison allows estimating the homogeneous broadening (see also [1]). The value  $\Gamma_v$  does not exceed  $1 \text{ cm}^{-1}$  at the vibrational energy levels  $E_v \approx 6000 \text{ cm}^{-1}$ . For more precise evaluation of  $\Gamma_v$  and its behaviour at the onset of vibrational quasi-continuum, the CARS spectra for higher temperatures are required. The comparison of experimental and calculated spectra will permit one to make a judgement on the distribution of molecules over vibrational states in the process of multiple photon excitation by infrared laser pulses.

*Acknowledgements.* The authors are indebted to Drs. R. V. Ambartsumian, N. I. Koroteev, A. A. Makarov for valuable discussions of this work.

## References

1. R.V. Ambartsumian, S.A. Akhmanov, A.M. Brodnikovskiy, S.M. Gladkov, A.V. Evseev, V.N. Zadkov, M.G. Karimov, N.I. Koroteev, A.A. Puzetzkyy: *JETP Lett.* **35**, 170 (1982)
2. S.S. Alimpiev, S.I. Valiansky, S.M. Nikiforov, V.V. Smirnov, B.G. Sartakov, V.I. Fabelinsky, A.L. Shtarkov: *JETP Lett.* **35**, 291 (1982)
3. I.N. Knyazev, V.A. Kudryavtsev, N.P. Kuzmina, V.S. Letokhov: *Sov. Phys. JETP* **49**, 650 (1979)
4. P.F. Moulton, A. Mooradian: *Opt. Lett.* **6**, 93 (1981)
5. J.W. Hudgens, J.D. McDonald: *J. Chem. Phys.* **76**, 173 (1982)
6. V.N. Bagratashvili, Yu.G. Vainer, V.S. Doljikov, S.F. Koliokov, A.A. Makarov, L.P. Malyavkin, E.A. Ryabov, E.G. Silkis, V.D. Titov: *Appl. Phys.* **22**, 101 (1980); *Opt. Lett.* **6**, 148 (1981)
7. S.A. Akhmanov, N.I. Koroteev: *Methods of Nonlinear Optics in Scattering Light Spectroscopy* (Nauka, Moscow 1981) (in Russian)
8. J.P. Taran: *Coherent Anti-Stokes Raman Spectroscopy*. In *Laser Spectroscopy III*, ed. by J.L. Hall, J.L. Carlsten (Springer, Berlin, Heidelberg, New York 1977)
9. A. Aboumjad, H. Berger, R. Saint-Loup: *J. Mol. Spectrosc.* **78**, 486 (1979)
10. W.B. Person, K.C. Kim: *J. Chem. Phys.* **69**, 2117 (1978)

11. K.C. Kim, W.B. Person, D. Seitz, B.J. Krohn: *J. Mol. Spectrosc.* **76**, 322 (1979)
12. A.S. Pine, C.W. Patterson: *J. Mol. Spectrosc.* **92**, 18 (1982)
13. P. Esherick, A. Owyong: *J. Mol. Spectrosc.* **92**, 162 (1982)
14. J. Cahen-Villard, M. Clers, P. Isnard, J.M. Weulersee: *J. Mol. Spectrosc.* **84**, 319 (1980)
15. M.A. Yuratich: *Mol. Phys.* **38**, 625 (1979)
16. A. Schultz, G. Marowsky: *Appl. Phys. B* **29**, 255–262 (1982)
17. Ch.J. Borde, M. Ouhayonn, A. Vanlerberghe, C. Salomon, S. Avrillier, C.D. Cantrell, J. Borde: In *Laser Spectroscopy IV*, ed. by H. Walther, K.W. Rothe (Springer, Berlin, Heidelberg, New York 1979) p. 142
18. R.S. McDowell, J.P. Aldridge, R.F. Holland: *J. Phys. Chem.* **80**, 1203 (1976)
19. A.S. Pine, A.G. Robiette: *J. Mol. Spectrosc.* **80**, 388 (1980)